INSTITUTE OF PHYSICS PUBLISHING JOURNAL OF PHYSICS: CONDENSED MATTER

J. Phys.: Condens. Matter **18** (2006) 5881–5894 doi:10.1088/0953-8984/18/26/008

Potential barrier for spin-polarized electrons induced by the exchange interaction at the interface in the ferromagnet/semiconductor heterostructure

L V Lutsev

Research Institute 'Ferrite-Domen', Chernigovskaya 8, Saint Petersburg, 196084, Russia

E-mail: lutsev@domen.ru

Received 7 February 2006, in final form 20 April 2006
Published 16 June 2006
Online at stacks.iop.org/JPhysCM/18/5881

Abstract
We have calculated the exchange interaction between electrons in the accumulation electron layer in the semiconductor near the interface and electrons in the ferromagnet in the ferromagnet/semiconductor heterostructure. It is found that the exchange interaction forms the potential barrier for spin-polarized electrons. The barrier height strongly depends on the difference of chemical potentials between the semiconductor and the ferromagnet. The maximum of the potential barrier height on the temperature dependence is due to the existence of localized electron states in the accumulation layer. In the framework of the developed theoretical model, the injection magnetoresistance effect observed in semiconductor/granular film heterostructures with ferromagnetic metal nanoparticles is explained. A spin filter on the base of granular film/semiconductor/granular film heterostructures operated at room temperature is proposed.

(Some figures in this article are in colour only in the electronic version)

1. Introduction

The interest in ferromagnet/semiconductor (FM/SC) interfaces is increasing due to the possibility of employing these structures as spin injectors of polarized electrons in SCs [1–3]. Transfer of spin-polarized electrons (spin injection) from a magnetic contact into a non-magnetic SC is intended for use in spintronic devices such as spin transistors, sensors and magnetic memory cells [4, 5]. It is noticed that the spin injection depends on a potential barrier formed at the interface. At present, the spin injection has been realized in heterostructures of different contact types.

(1) Spin injection from a magnetic SC into a non-magnetic SC is observed at low temperatures [6–8]. But at room temperature spin-polarized transport effects are small or disappear.

(2) Injection of spin-polarized electrons from a ferromagnetic metal into an SC is experimentally investigated and reveals low spin injection efficiency [9–14]. Low values of the efficiency result from the conductivity mismatch between the injecting and receiving materials [5, 15]. Moreover, in ferromagnetic metals the electron concentration of conduction electrons is high and the s–d (s–f) exchange interaction is shielded by electrons of the conduction band. This results in low values of the spin polarization of the current (1–10%) [16, 17]. At the same time, we need to notice that Schottky-type contacts formed at the ferromagnetic metal/SC interface can lead to an enhanced spin injection efficiency.
(3) Spin injection in the ferromagnetic metal/insulator/SC heterostructure is more efficient in comparison with the spin injection from a ferromagnetic metal into an SC with a Schottky barrier [18–21]. The maximum of the spin polarization of injected electrons is achieved for an MgO barrier on GaAs (57% at 100 K and 47% at 290 K) [20].

Although significant progress has been made, the efficient spin injection has not been achieved and the highly efficient spin injection into SCs at room temperature is the actual problem. This problem can be resolved by using FM/SC heterostructures with an accumulation electron layer in the SC at the interface. The exchange interaction between d (f) electrons in the FM at the interface and electrons in the SC polarizes electrons in the accumulation layer. This interaction forms a potential barrier for spin-polarized electrons injected from the FM. In this paper, we study the potential barrier induced by the exchange interaction. We have found that the existence of localized electron states at the interface in the SC leads to the increase of the effective exchange interaction, and, in this case, the potential barrier height has a maximum. The barrier height strongly depends on the difference of chemical potentials between the SC and the FM.

Using the developed theoretical model, we propose spin injectors on the basis of FM/SC heterostructures and spin filters based on FM/SC/FM heterostructures, where the FM is the granular film of an insulator with ferromagnetic metal nanoparticles. Due to the granular film in these heterostructures, accumulation layers at interfaces are formed. We consider the case of the first heterostructure, namely, GaAs/SiO_2 granular film with Co nanoparticles, where the effect of the positive injection magnetoresistance has been observed, and explain experimental results of the magnetoresistance [22, 23]. In this heterostructure the injection magnetoresistance reaches 5200% at room temperature. This shows that the heterostructures with granular films are highly efficient materials for spin filters and spin aligners.

2. Theoretical model

Let us consider an interface of the FM/SC structure with an accumulation electron layer (figure 1). We assume that the FM has unpaired d electrons, and the d electrons determine magnetic characteristics of the FM. In the common case, chemical potentials of the FM and the SC, considered as separated solids, differ. In the heterostructure the difference of chemical potentials $\Delta\mu$ between the FM and the SC determines bending of the SC conduction band. We assume that (1) bending leads to the formation of an accumulation layer and (2) d electrons in the FM at the interface and electrons in the accumulation electron layer in the SC are coupled by the exchange interaction $J_0(\vec{r}-\vec{R})$. We write the Hamiltonian of the model in the form

$$\mathcal{H} = \mathcal{H}_{\mathrm{e}} + \mathcal{H}_{\mathrm{ed}} + \mathcal{H}_{\varphi}, \tag{1}$$

where

$$\mathcal{H}_{\mathrm{e}} = \sum_{\alpha} \int \Psi_{\alpha}^{+}(\vec{r}) \left[-\frac{\hbar^2}{2m}\Delta - \mu - e\varphi(\vec{r}) \right] \Psi_{\alpha}(\vec{r})\, \mathrm{d}\vec{r}$$

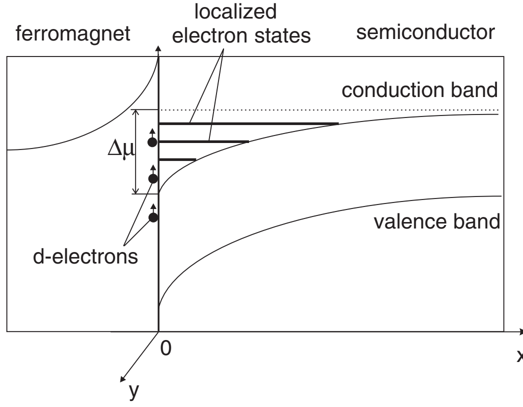

Figure 1. Electronic energy band structure at the contact region of the ferromagnet/semiconductor.

is the Hamiltonian of electrons in the SC in the electrical field with the potential $\varphi(\vec{r})$. m is the electron mass. e is the electron charge. μ is the chemical potential. $\Psi^+_\alpha(\vec{r}) = \sum_\lambda \psi^*_\lambda(\vec{r})a^+_{\lambda\alpha}$, $\Psi_\alpha(\vec{r}) = \sum_\lambda \psi_\lambda(\vec{r})a_{\lambda\alpha}$ are the second-quantized wavefunctions of an electron. $a^+_{\lambda\alpha}$, $a_{\lambda\alpha}$ are the creation and annihilation Fermi operators, respectively, for an electron at the energy level λ of the one-particle state with a spin $\alpha = \uparrow, \downarrow$. We assume that the axis Ox is normal to the interface plane and $\vec{r} = (x, y, z)$. Thus, in the given coordinate system the wavefunction $\psi_\lambda(\vec{r}) = V^{-1/2}\chi_\nu(x)\exp(\mathrm{i}q_y y + \mathrm{i}q_z z)$ of an electron in the volume V of the SC with the multiindex $\lambda = (\nu, q_y, q_z)$ and the energy spectrum $\varepsilon_\lambda = \varepsilon^{(0)}_\nu + \hbar^2(q_y^2 + q_z^2)/2m$ of the one-particle state are determined by the equation

$$\left[-\frac{\hbar^2}{2m}\frac{\mathrm{d}^2}{\mathrm{d}x^2} - e\varphi(x)\right]\chi_\nu(x) = \varepsilon^{(0)}_\nu\chi_\nu(x). \tag{2}$$

In the common case, equation (2) determines localized electron states with discrete spectrum and non-localized states with continuous spectrum (figure 1). We assume that electrons in the SC penetrate into the FM in an infinitesimally thin layer, in which d electrons are localized, so $\chi'_\nu(0) = 0$ and $\chi_\nu(0) \neq 0$. At $x < 0$ outside the infinitesimally thin layer the wavefunction $\chi_\nu(x) = 0$.

$$\mathcal{H}_{\mathrm{ed}} = -\sum_{\vec{R}}\int J_0(\vec{r} - \vec{R})(\vec{S}(\vec{R}), \vec{\sigma}(\vec{r}))\,\mathrm{d}\vec{r}$$

is the exchange interaction Hamiltonian between the spin density $\vec{\sigma}(\vec{r})$ of electrons in the SC and spins of d electrons in the FM. $\vec{S}(\vec{R})$ is the vector spin operator of a d electron on the site $\vec{R}$. The vector spin density operator $\vec{\sigma}(\vec{r})$ is determined by operators $\Psi_\alpha(\vec{r})$, $\Psi^+_\alpha(\vec{r})$

$$\sigma_x(\vec{r}) = \Psi^+_\uparrow(\vec{r})\Psi_\downarrow(\vec{r}) + \Psi^+_\downarrow(\vec{r})\Psi_\uparrow(\vec{r})$$
$$\sigma_y(\vec{r}) = -\mathrm{i}\Psi^+_\uparrow(\vec{r})\Psi_\downarrow(\vec{r}) + \mathrm{i}\Psi^+_\downarrow(\vec{r})\Psi_\uparrow(\vec{r})$$
$$\sigma_z(\vec{r}) = \Psi^+_\uparrow(\vec{r})\Psi_\uparrow(\vec{r}) - \Psi^+_\downarrow(\vec{r})\Psi_\downarrow(\vec{r}).$$

The term

$$\mathcal{H}_\varphi = -\frac{1}{8\pi}\int[\nabla\varphi(\vec{r})]^2\,\mathrm{d}\vec{r}$$

is the Hamiltonian of the classical inner electrostatic field.

The system described by the Hamiltonian $\mathcal{H}$ in relation (1) is in the thermodynamic equilibrium state and is characterized by temperature T. In order to find properties of this system, we use the temperature diagram technique [24, 25]. We will calculate values of energy

a.

$G_{\lambda\uparrow\uparrow}(\boldsymbol{r}_1, \boldsymbol{r}_2, \omega_n) =$

$G_{\lambda\downarrow\downarrow}(\boldsymbol{r}_1, \boldsymbol{r}_2, \omega_n) =$

b.

$\beta J_0(\boldsymbol{r}-\boldsymbol{R}) =$

$\beta J^{(eff)}(\boldsymbol{r}, \boldsymbol{R}, \omega_n) = \; + \; + $

c.

$\langle \sigma_z^{(p)}(\boldsymbol{r}) \rangle = \quad \langle S_z(\boldsymbol{R}) \rangle_0 =$

$W = \sum_{\boldsymbol{R}} \int \langle \sigma_z^{(p)}(\boldsymbol{r}) \rangle \, J^{(eff)}(\boldsymbol{r}, \boldsymbol{R}, 0) \, \langle S_z(\boldsymbol{R}) \rangle_0 \, d\boldsymbol{r} =$

$= \beta^{-1} \{ \; + \; + \; \}$

Figure 2. (a) Temperature electron Green functions with the spin ↑ and ↓. (b) Bare and effective exchange interactions. (c) Potential barrier W induced by the effective exchange interaction.

barriers formed by the effective exchange interaction in the accumulation layer in the one-loop approximation with respect to the bare exchange interaction $J_0(\vec{r} - \vec{R})$ for a diagram expansion of the effective interaction. The diagram technique for our model is analogous to the diagram technique for the s–d-exchange model, which is described in [24, 26, 27]. In the self-consistent-field approximation in terms of the eigenfunctions $\psi_\lambda(\vec{r})$ of the Hamiltonian $\mathcal{H}_e$, the Fourier transform of the temperature electron Green functions $\langle T_\tau \tilde{\Psi}^+_{\alpha_1}(\vec{r}_1, \tau_1) \tilde{\Psi}_{\alpha_2}(\vec{r}_2, \tau_2) \rangle_0$ (where $\tilde{\Psi}_\alpha(\vec{r}, \tau) = \exp(\mathcal{H}\tau) \Psi_\alpha(\vec{r}) \exp(-\mathcal{H}\tau)$, T_τ is the temperature ordering operator, $\tau \in [0, \beta]$, $\beta = 1/kT$, k is the Boltzmann constant) has the form [25]

$$G_{\lambda\alpha_1\alpha_2}(\vec{r}_1, \vec{r}_2, \omega_n) = \frac{\psi^*_\lambda(\vec{r}_1)\psi_\lambda(\vec{r}_2)\delta_{\alpha_1\alpha_2}}{\beta(\mathrm{i}\hbar\omega_n - E_{\lambda\alpha} + \mu)}, \tag{3}$$

where $\hbar\omega_n = (2n+1)\pi/\beta$, n is an integer,

$$E_{\lambda\alpha} = \varepsilon_\lambda \mp \varepsilon_\lambda^{(\mathrm{exch})}. \tag{4}$$

The upper sign in equation (4) corresponds to $\alpha = \uparrow$, the lower sign to $\alpha = \downarrow$. The energy $\varepsilon_\lambda^{(\mathrm{exch})}$ is determined by the exchange Hamiltonian $\mathcal{H}_{\mathrm{ed}}$ in the self-consistent-field approximation

$$\varepsilon_\lambda^{(\mathrm{exch})} = -\sum_{\vec{R}} \int J_0(\vec{r} - \vec{R})(\langle \vec{S}(\vec{R}) \rangle_0, \langle \vec{\sigma}(\vec{r}) \rangle_0) \, \mathrm{d}\vec{r}. \tag{5}$$

$\langle \vec{S}(\vec{R}) \rangle_0$ and $\langle \vec{\sigma}(\vec{r}) \rangle_0$ are the statistical-average d-electron spin in the FM and the electron spin density in the SC, respectively. Since the exchange interaction is isotropic, without loss of generality we assume that $\langle \vec{S}(\vec{R}) \rangle_0$ is parallel to the axis Oz. The exchange interaction splits an electronic level into two. The bare Green functions in relation (3) are represented by directed lines in diagrams (figure 2(a)).

The equation for the inner self-consistent electrical field is derived from the variation of the action determined by the Hamiltonians $\mathcal{H}_e$, $\mathcal{H}_\varphi$ in (1) in the potential $\varphi(\vec{r})$. The action is obtained by statistical averaging $\langle\cdots\rangle_0$ with the temperature ordering operator T_τ and its minimum is achieved at the potential $\varphi(\vec{r})$, which is given by the equation

$$\Delta\varphi(\vec{r}) = 4\pi e\left\{\sum_{\lambda,\omega_n}[G_{\lambda\uparrow\uparrow}(\vec{r},\vec{r},\omega_n) + G_{\lambda\downarrow\downarrow}(\vec{r},\vec{r},\omega_n) - G^{(0)}_{\lambda\uparrow\uparrow}(\vec{r},\vec{r},\omega_n) - G^{(0)}_{\lambda\downarrow\downarrow}(\vec{r},\vec{r},\omega_n)]\right\}, \tag{6}$$

where $G_{\lambda\alpha\alpha}$ are electron Green functions, expressed by relation (3), and $G^{(0)}_{\lambda\alpha\alpha}$ are electron Green functions determined in the single SC in the absence of the electrical field. If the heterostructure FM/SC is homogeneous over axes y and z, equation (6) can be simplified. In this case, after performing the summation over ω_n, equation (6) is written in the form

$$\frac{\mathrm{d}^2\varphi(x)}{\mathrm{d}x^2} = 4\pi e\left\{\sum_{\lambda=(\nu,q_y,q_z)}\big[n_F[\beta(\varepsilon_\lambda - \varepsilon^{(\mathrm{exch})}_\lambda - \mu)] + n_F[\beta(\varepsilon_\lambda + \varepsilon^{(\mathrm{exch})}_\lambda - \mu)]\big]\,|\chi_\nu(x)|^2/V - n_0\right\}, \tag{7}$$

where $n_F(a) = [\exp(a)+1]^{-1}$, n_0 is the electron concentration in the single SC, when the SC is not contacted with the FM. At the interface of the heterostructure ($x = 0$) the potential $\varphi(x)$ is determined by the difference of chemical potentials $\Delta\mu$ between the SC and the FM: $\varphi(0) = \Delta\mu/e$. At a great distance from the interface, when $x \to \infty$, the potential $\varphi(x)$ tends to zero. Taking into account that in the single SC the electrical potential $\varphi(x) = 0$, the wavefunction $\chi_\nu(x) = \exp(\mathrm{i}q_x x)$, the energies $\varepsilon^{(0)}_\nu = \hbar^2 q_x^2/2m$ for $\nu = q_x$ and $\varepsilon^{(\mathrm{exch})}_\lambda = 0$ for $\lambda = (q_x, q_y, q_z)$, from equation (7) we obtain a relationship between the chemical potential μ and the electron concentration n_0 in the single SC

$$n_0 = \frac{8\pi e}{V}\sum_{\vec{q}=(q_x,q_y,q_z)} n_F[\beta(\hbar^2|\vec{q}|^2/2m - \mu)]. \tag{8}$$

Equations (2), (7) and (8) are simultaneous equations in unknowns: the wavefunction $\chi_\nu(x)$, the energy $\varepsilon^{(0)}_\nu$, the electrical potential $\varphi(x)$, and the chemical potential μ in the SC. Solutions of these equations are necessary for determination of the effective exchange interaction $J^{(\mathrm{eff})}(\vec{r},\vec{R},\omega_n)$ between the spin density $\langle\sigma_z^{(p)}(\vec{r})\rangle$ of a probe (injected) electron and the d-electron spin $\langle S_z(\vec{R})\rangle_0$. The effective exchange interaction is found in the one-loop approximation with respect to the bare exchange interaction $J_0(\vec{r}-\vec{R})$ (figure 2(b))

$$J^{(\mathrm{eff})}(\vec{r},\vec{R},\omega_n) = J_0(\vec{r}-\vec{R}) + J_1(\vec{r},\vec{R},\omega_n),$$

where the exchange interaction J_1 (the RKKY-type interaction) has the form

$$\begin{aligned}J_1(\vec{r},\vec{R},\omega_n) &= -\beta\int\!\!\int J_0(\vec{r}-\vec{r}_1)\sum_{k,\lambda_1,\lambda_2}[G_{\lambda_1\uparrow\uparrow}(\vec{r}_1,\vec{r}_2,\omega_k)G_{\lambda_2\uparrow\uparrow}(\vec{r}_2,\vec{r}_1,\omega_k+\omega_n)\\ &\quad + G_{\lambda_1\downarrow\downarrow}(\vec{r}_1,\vec{r}_2,\omega_k)G_{\lambda_2\downarrow\downarrow}(\vec{r}_2,\vec{r}_1,\omega_k+\omega_n)]J_0(\vec{r}_2-\vec{R})\,\mathrm{d}\vec{r}_1\,\mathrm{d}\vec{r}_2\\ &= \frac{1}{V^2}\int\!\!\int J_0(\vec{r}-\vec{r}_1)\sum_{\substack{\alpha=\uparrow,\downarrow\\ \lambda_1=(\nu_1 q_{1y} q_{1z})\\ \lambda_2=(\nu_2 q_{2y} q_{2z})}}\frac{n_F[\beta(E_{\lambda_2\alpha}-\mu)] - n_F[\beta(E_{\lambda_1\alpha}-\mu)]}{\varepsilon_{\lambda_2}-\varepsilon_{\lambda_1}-\mathrm{i}\hbar\omega_n}\\ &\quad\times J_0(\vec{r}_2-\vec{R})\exp[\mathrm{i}(q_{1y}-q_{2y})(y_2-y_1)+\mathrm{i}(q_{1z}-q_{2z})(z_2-z_1)]\\ &\quad\times \chi^*_{\nu_1}(x_1)\chi_{\nu_1}(x_2)\chi_{\nu_2}(x_1)\chi^*_{\nu_2}(x_2)\,\mathrm{d}\vec{r}_1\,\mathrm{d}\vec{r}_2.\end{aligned} \tag{9}$$

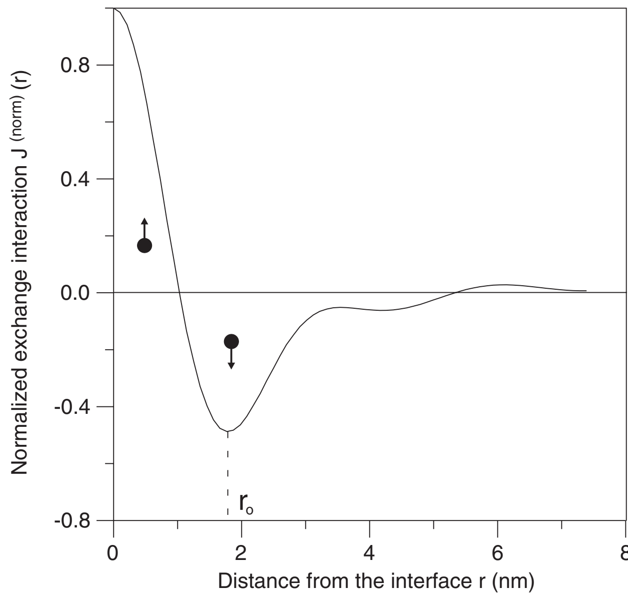

Figure 3. Normalized exchange interaction $J^{(\mathrm{norm})}(r)$ for the heterostructure with the difference of chemical potentials $\Delta\mu = 150$ meV and with the electron concentration $n_0 = 1 \times 10^{15}$ cm^{-3} in the SC at $T = 300$ K.

Energies $E_{\lambda_i\alpha}$ are determined by equation (4). The wavefunctions $\chi_{\nu_i}(x_j)$, energies ε_{λ_i}, the electrical potential $\varphi(x)$ and the chemical potential μ in the SC must be found as solutions of simultaneous equations (2), (7) and (8). The numerical solution of these equations and the calculation of the exchange interaction J_1, expressed by equation (9), are found for various values of the difference of chemical potentials $\Delta\mu$ between the SC and the FM, and for various values of temperature T. We assume that $J_0(\vec{r} - \vec{R}) = J_0 \exp(-\xi|\vec{r} - \vec{R}|)$ in equations (5) and (9), where ξ is the reciprocal radius of the exchange interaction. Calculations have been drawn, when $\omega_n = 0$, $\vec{R} = 0$ in equation (9), and $\xi = 10$ nm^{-1}, $J_0 = 2$ eV, $|\langle\vec{S}(\vec{R})\rangle_0| = 1/2$, $|\langle\vec{\sigma}(\vec{r})\rangle_0| = 1/2|\psi_\lambda(\vec{r})|^2$ in equations (5), (9). We assume that the FM has the cubical crystal lattice with the lattice constant $a = 0.23$ nm. For this lattice the magnetization $4\pi M = 4\pi g\mu_{\mathrm{B}}|\langle\vec{S}\rangle_0|/a^3$ is equal to 10 kOe. g and μ_{B} are the Landé factor and the Bohr magneton, respectively. The calculated normalized interaction $J^{(\mathrm{norm})}(r) = J_1(\vec{r}, \vec{R}, \omega_n)/J_1(0, \vec{R}, \omega_n)$ for $\vec{r} = (r, 0, 0)$, $\omega_n = 0$, $\vec{R} = 0$ is presented in figure 3 for the heterostructure with $\Delta\mu = 150$ meV, $n_0 = 1 \times 10^{15}$ cm^{-3} at $T = 300$ K. It can be seen that the exchange interaction changes its sign at $r > 1.0$ nm.

The height of the energy barrier formed by the effective exchange interaction is determined by the relation (figure 2(c))

$$W = \sum_{\vec{R}} \int \langle\sigma_z^{(p)}(\vec{r})\rangle J^{(\mathrm{eff})}(\vec{r}, \vec{R}, 0)\langle S_z(\vec{R})\rangle_0 \, \mathrm{d}\vec{r} \tag{10}$$

for the spin density $\langle\sigma_z^{(p)}(\vec{r})\rangle = 1/2 \cdot \delta(r - r_0)$ at the distance r_0 from the interface, where the exchange interaction J_1 has a maximum opposite value (figure 3). Figure 4 shows the energy barrier W versus the difference of chemical potentials $\Delta\mu$ between the SC and the FM with the electron concentration $n_0 = 1 \times 10^{15}$ cm^{-3} in the SC at $T = 300$ K. It can be seen that the height of the energy barrier has a maximum value at $\Delta\mu = 220$ meV. The maximum of the barrier is due to the presence of localized electron states at the interface. We have found that localized states $\chi_\nu(x)$, which are determined by equation (2), give the main contribution to the exchange interaction J_1 in equation (9). If the difference $\Delta\mu$ is small, the accumulation well is shallow and wide. This results in a low electron concentration at the interface and gives low

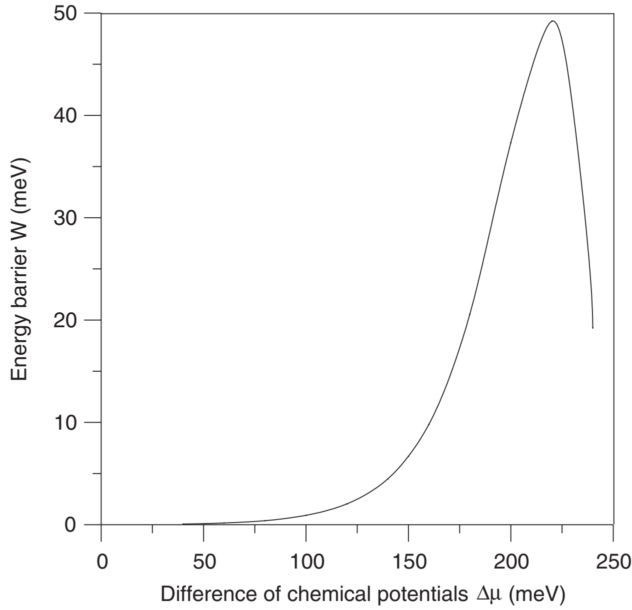

Figure 4. Potential barrier height W versus the difference of chemical potentials $\Delta\mu$ in the heterostructure at $T = 300$ K. The electron concentration n_0 in the SC is equal to 1×10^{15} cm^{-3}.

values of the barrier height W. If the difference $\Delta\mu$ is greater than 220 meV, the accumulation well is thin. Despite the fact that the electron concentration at the interface is high, the number of localized electron states in the thin well sharply decreases with decreasing thickness. If the accumulation well does not contain localized states, the magnitude of W falls. The maximum of the barrier is observed when the accumulation well has a small number of localized electron states. For the maximum height of the barrier, the electron concentration at the interface is equal to 0.66×10^{19} cm^{-3}.

The temperature dependences of the potential barrier W are presented in figure 5 for heterostructures with the electron concentration $n_0 = 1 \times 10^{15}$ cm^{-3} (at $T = 300$ K) in the SC with various values of the difference of chemical potentials $\Delta\mu$. At the interface the electron concentration increases with temperature increasing. At low temperatures this causes the growth of the barrier W. At a certain temperature the magnitude of W reaches the maximum value. The further temperature growth gives higher electron concentrations at the interface and results in the thin accumulation well with a small number of localized electron states. As a result of the decrease of the number of localized states and their further disappearance with decreasing thickness of the accumulation well, the height of the potential barrier decreases.

We have considered the potential barrier forming in the FM/non-magnetic SC heterostructure. The developed theory can be generalized on FM/dilute magnetic SC heterostructures. In this case, the exchange interaction Hamiltonian in relation (1) is the sum of two terms

$$\mathcal{H}_{\rm ed} = -\sum_{\vec{R}} \int J_0^{\rm (FM)}(\vec{r} - \vec{R})(\vec{S}^{\rm (FM)}(\vec{R}), \vec{\sigma}(\vec{r}))\,{\rm d}\vec{r} - \sum_{\vec{\rho}} \int J_0^{\rm (MI)}(\vec{r} - \vec{\rho})(\vec{S}^{\rm (MI)}(\vec{\rho}), \vec{\sigma}(\vec{r}))\,{\rm d}\vec{r},$$

where $J_0^{\rm (FM)}$ is the exchange interaction between the spin density $\vec{\sigma}(\vec{r})$ of electrons in the SC and spins of d electrons $\vec{S}^{\rm (FM)}(\vec{R})$ in the FM at the interface; $J_0^{\rm (MI)}$ is the exchange interaction between the spin density $\vec{\sigma}(\vec{r})$ of electrons in the SC conduction band and spins of magnetic ions $\vec{S}^{\rm (MI)}(\vec{\rho})$ in the dilute magnetic SC. The summation is performed over sites $\vec{R}$ of d-electron spins in the FM and over sites $\vec{\rho}$ of spins of magnetic ions in the dilute magnetic SC. The

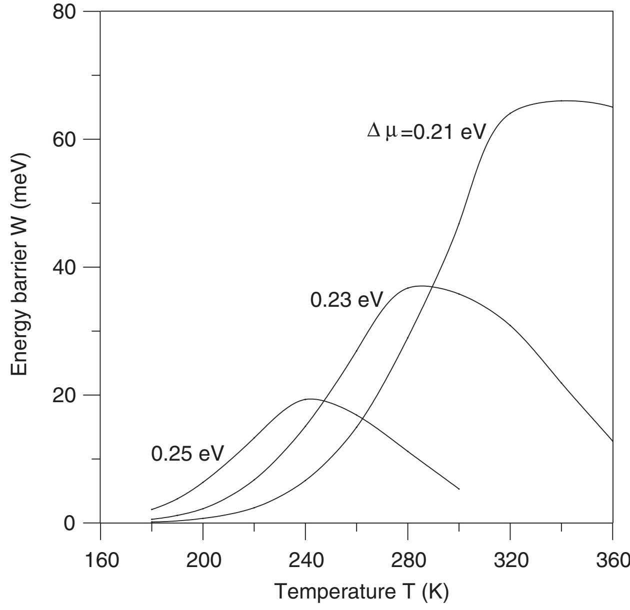

Figure 5. Temperature dependences of the potential barrier height W for heterostructures with the difference of chemical potentials $\Delta\mu = 0.21$; 0.23; 0.25 eV. The electron concentration n_0 in the SC is equal to 1×10^{15} cm^{-3} at $T = 300$ K.

modification of the Hamiltonian $\mathcal{H}_{\mathrm{ed}}$ leads to the modification of the exchange energy $\varepsilon_\lambda^{(\mathrm{exch})}$ in relation (5). In this case, the exchange energy is given by the form

$$\varepsilon_\lambda^{(\mathrm{exch})} = -\sum_{\vec{R}} \int J_0^{(\mathrm{FM})}(\vec{r} - \vec{R})(\langle \vec{S}^{(\mathrm{FM})}(\vec{R})\rangle_0, \langle \vec{\sigma}(\vec{r})\rangle_0)\,\mathrm{d}\vec{r} - \sum_{\vec{\rho}} \int J_0^{(\mathrm{MI})}(\vec{r} - \vec{\rho})(\langle \vec{S}^{(\mathrm{MI})}(\vec{\rho})\rangle_0, \langle \vec{\sigma}(\vec{r})\rangle_0)\,\mathrm{d}\vec{r}.$$

After these changes we can use equations (2), (7) and (8) to find the wavefunction $\chi_\nu(x)$, the energy $\varepsilon_\nu^{(0)}$, the electrical potential $\varphi(x)$, and the chemical potential μ in the dilute magnetic SC. The effective exchange interaction induced by d electrons in the FM at the interface and the energy barrier W formed by this interaction are determined by the same equations (9) and (10), respectively.

3. Injection magnetoresistance and spin filters

According to the developed theoretical model, it follows that the potential barrier for spin-polarized electrons in the accumulation electron layer in the SC is formed when the chemical potential μ_{s} in the SC has lower values than the chemical potential μ_{f} in the FM. In the case when the FM is a d or f ferromagnetic metal, as a rule, this relation is not held, i.e. $\mu_{\mathrm{s}} > \mu_{\mathrm{f}}$, and the depletion layer and the Schottky barrier are formed in the SC. In order to overcome this discrepancy and to obtain the accumulation electron layer, we use granular structures as the FM. Granular structures consist of an insulator matrix and embedded ferromagnetic metal nanoparticles. In the first approximation, the chemical potential μ_{g} of granular structures is given by

$$\mu_{\mathrm{g}} = \mu_{\mathrm{i}} x_{\mathrm{i}} + \mu_{\mathrm{fm}} x_{\mathrm{fm}}, \tag{11}$$

where μ_{i} and μ_{fm} are the chemical potentials of the insulator matrix and the ferromagnetic metal; x_{i} and x_{fm} are the atomic concentrations of the insulator and the metal, respectively. As

a rule, $\mu_s < \mu_i$ and we can fulfil the inequality $\mu_s < \mu_g$ by usage of the proper type of the insulator. Moreover, we can choose the value of the conductivity of the granular structure equal to the SC conductivity to overcome the conductivity mismatch. We need to notice that the small size of ferromagnetic metal nanoparticles is a necessary condition to use the granular structures. The developed theory can be applied for the granular structure/SC, if the size of metal nanoparticles is less than the thickness l of the accumulation layer. In this case, the granular structure can be characterized by average parameters and the thickness l can be determined by the difference of the chemical potentials $\Delta\mu = \mu_g - \mu_s$.

Let us consider SC/granular film heterostructures with ferromagnetic metal nanoparticles and granular film/SC/granular film heterostructures. On the first heterostructures the effect of the injection magnetoresistance has been observed in experiments [22, 23]. The second heterostructures can be used as effective spin filters.

3.1. Injection magnetoresistance in semiconductor/granular film heterostructures

A new phenomenon, injection magnetoresistance, has been observed in GaAs/SiO_2 granular film with Co nanoparticles [22, 23]. The injection magnetoresistance is the suppression of the electron injection from the granular film into GaAs induced by the magnetic field. It is found that the injection magnetoresistance effect reaches the maximum at a certain temperature and becomes less pronounced as the temperature decreases. This effect depends strongly on the Co content in the SiO_2(Co) granular film deposited on the GaAs substrate. The observed injection magnetoresistance reaches 5200% at room temperature. This magnetoresistance value is two orders of magnitude higher than the values of the giant magnetoresistance and tunnelling magnetoresistance that are observed in layered metallic and magnetic tunnelling structures.

In the experiments, which have been carried out in [22, 23], the carrier concentration in the n-GaAs is equal to 1×10^{15} cm^{-3}. The size of Co nanoparticles in the granular film is 2.7–3.5 nm in the Co concentration range 39–60 at.%. This heterostructure is satisfied with the above-mentioned conditions of small sizes of metal nanoparticles, and the inequality $\mu_s < \mu_g$ can be held. The difference $\Delta\mu$ between chemical potentials of the GaAs and the granular film can be estimated from well known values of the energy of the thermoelectron emission. For the given materials the differences of the chemical potentials are $\mu_{SiO_2} - \mu_{GaAs} = 0.62$ eV and $\mu_{Co} - \mu_{GaAs} = 0.03$ eV [28]. This leads to lowering the conduction band in the GaAs in regions of SC/granular film contacts and forms an accumulation electron layer in the GaAs near the interface (figure 6).

The geometry of samples is shown in figure 7. The sample size L is 3 mm; the thickness d of the SC is 0.4 mm. One contact is on the GaAs substrate, and the other on the granular film. The resistivity of the granular film is determined by the inelastic resonance electron tunnelling via localized states, which are formed in the dielectric SiO_2 matrix between isolated conducting metal clusters [29–31]. For the samples with a high Co content ($x_{Co} > 55$ at.%), the resistivity of GaAs is higher than the resistivity of the film and the applied voltage primarily falls on the SC. In order to estimate the suppression of the electron injection induced by the magnetic field, the injection magnetoresistance coefficient, IMR, is introduced

$$\mathrm{IMR} = \frac{R(H) - R(0)}{R(0)} = \frac{j(0) - j(H)}{j(H)}, \tag{12}$$

where $R(0)$ and $R(H)$ are the resistances of the heterostructure, and $j(0)$ and $j(H)$ are the injection current densities in the absence and in the presence of the magnetic field H, respectively. The IMR coefficient increases with increasing magnetic field and is saturated in high magnetic fields. For the investigated heterostructure with 60 at.% Co, the injection magnetoresistance has a maximum (5200%) in the magnetic field $H = 23$ kOe at room

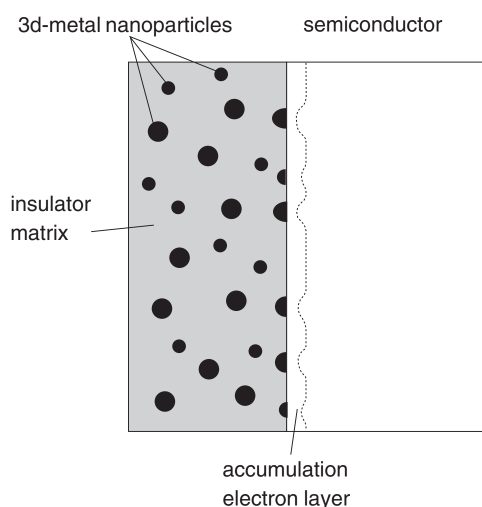

Figure 6. Accumulation layer in the SC/granular film heterostructure with ferromagnetic metal nanoparticles.

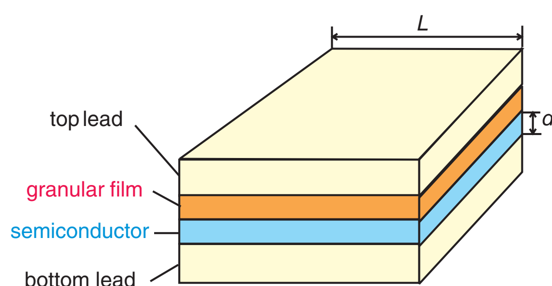

Figure 7. Geometry of samples of SC/granular film heterostructures with ferromagnetic metal nanoparticles, which are used in injection magnetoresistance experiments.

temperature. For heterostructures with a lower or higher content of Co, the IMR coefficient sharply decreases. It is found that the IMR coefficient has a maximum on the temperature dependence.

The observed injection magnetoresistance effect can be explained by the developed theory. For the explanation it is essential that (1) the domain structure is experimentally observed in the granular film [23] and (2) the potential barrier is formed in the accumulation electron layer in the SC at the distance r_0 from the interface plane (figure 3). Due to the RKKY interaction between d electrons of neighbouring Co particles, which are close to the interface, and electrons of the accumulation layer in the SC, ferromagnetic metal particles with electrons of the accumulation layer form a ferromagnetic layer (figure 8). In the absence of an external magnetic field, the domain structure of the ferromagnetic layer at the interface induces corresponding spin orientations of electrons localized in the accumulation layer and this domain structure has domain walls. In this case, electrons injected from the granular film can cross through the accumulation layer without a loss of their spin polarization and without surmounting the potential barrier on channels close to domain walls (figure 8). In the magnetic field of high values, when the saturation limit is reached and domains disappear, spin-polarized electrons moving in the SC from the interface must surmount the potential barrier at the distance r_0. The current density j of injected electrons is determined by the concentration of injected electrons n and by the average velocity v, which is expressed by the kinetic energy $E^{(\mathrm{kin})}$ of electrons in the region of the potential barrier: $j = env = en(2E^{(\mathrm{kin})}/m)^{1/2}$. We assume that the potential barrier is not tunnel transparent. Then, taking into account equation (12), we find that in the

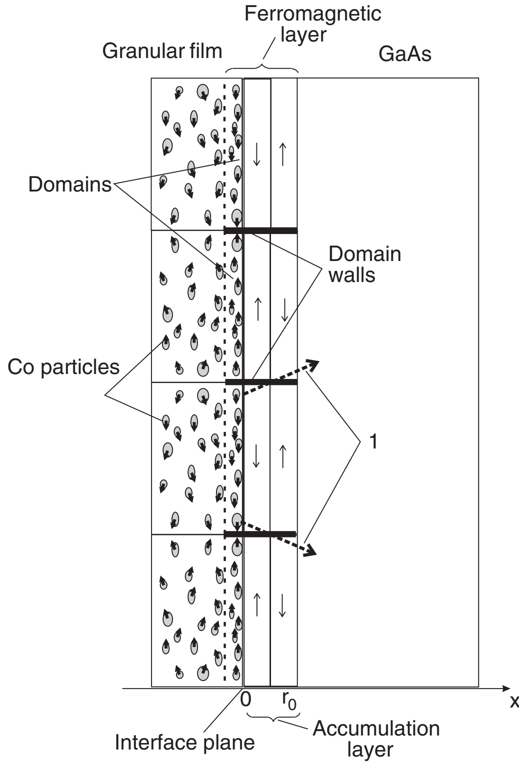

Figure 8. Paths (1) without spin-flip scattering of injected electrons on the accumulation layer for the case when the ferromagnetic layer has domain structure in the absence of a magnetic field. ↑ and ↓ denote spin polarization of injected electrons in the accumulation layer, where they have lowest potential energies.

magnetic field of high values, when the IMR coefficient is saturated, the maximum magnitude of the IMR as a function of W is given by

$$\max \mathrm{IMR}(W) = \frac{n_0 v_0 - n_s v_s}{n_s v_s}, \tag{13}$$

where $v_0 = (2/m)^{1/2} \int_{-W}^{\infty} (E + W)^{1/2} \rho(E)\, dE$, $v_s = (2/m)^{1/2} \int_{W}^{\infty} (E - W)^{1/2} \rho(E)\, dE$ are the average value of the electron velocity in conductivity channels close to domain walls in the absence of a magnetic field and the average value of the electron velocity in the barrier region in the magnetic field of high values, respectively; $n_0 = \int_{-W}^{\infty} \rho(E)\, dE$, $n_s = \int_{W}^{\infty} \rho(E)\, dE$ are the concentrations of injected electrons in conductivity channels in the absence of a magnetic field and in the barrier region in the magnetic field, respectively; $\rho(E)$ is the energy distribution of injected electrons; E is the electron energy counted from the bottom of the conduction band of the SC at the distance r_0 in the non-exchange approximation. From equation (13) we find that, if the energy distribution $\rho(E)$ is a slowly varying, decreasing function of E, then in the first approximation the IMR coefficient is proportional to the barrier height W.

The experimental temperature dependence of the IMR coefficient for the $SiO_2(Co)/GaAs$ structure with $x_{Co} = 60$ at.% has a maximum at $T = 280$ K (figure 9) [22, 23]. As a function of T, the experimental temperature dependence is proportional to the calculated temperature dependence of the potential barrier height W for the SC/granular film heterostructure with the difference of chemical potentials $\Delta\mu = 0.23$ eV (figure 5).

In the experiment the IMR coefficient strongly depends on the Co content in the granular film [22]. The IMR coefficients for the $SiO_2(Co)/GaAs$ heterostructure with the Co concentration 60 at.% and for heterostructures with $x_{Co} = 39$ and 85 at.% differ by two orders of magnitude at high magnetic fields. In accordance with the relation (11), the growth of the Co

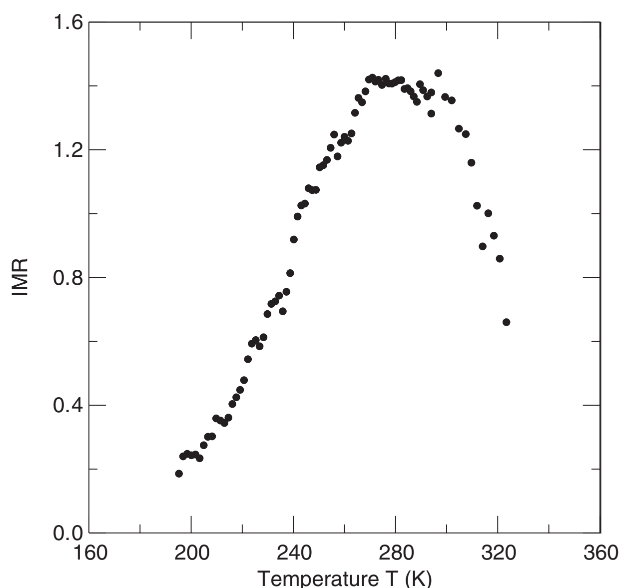

Figure 9. The injection magnetoresistance coefficient IMR for the $SiO_2(Co)/GaAs$ structure with 60 at.% Co at the voltage $U = 35$ V in the magnetic field $H = 2.6$ kOe (from paper [22]).

content results in decreasing the difference of chemical potentials $\Delta\mu = \mu_g - \mu_s$. According to the above-mentioned temperature dependence of IMR and W, the difference $\Delta\mu$ is equal to 0.23 eV for the heterostructure with $x_{Co} = 60$ at.%. Therefore, for the heterostructure with $x_{Co} = 39$ at.% the difference $\Delta\mu$ is greater than 0.23 eV, and for the heterostructure with $x_{Co} = 85$ at.% the difference $\Delta\mu$ is less than 0.23 eV. Taking into account the potential barrier height W versus the difference of chemical potentials $\Delta\mu$ shown in figure 4, we find that the experimentally observed maximum of the coefficient IMR coincides with the maximum of the barrier height at $\Delta\mu = 0.23$ eV and the theoretical dependence of the height W on the difference $\Delta\mu$ confirms the experimental results.

3.2. Spin filters on the base of granular film/semiconductor/granular film heterostructures

The injection of spin-polarized electrons in SC/granular film heterostructures is governed by the potential barrier at the distance r_0 from the interface in the accumulation layer of the SC (figures 3, 8). More efficient manipulation of spin-polarized currents can be obtained in granular film/SC/granular film heterostructures (figure 10). In this case, two SC/granular film interfaces and two accumulation electron layers are formed. If the thickness d of the SC is much greater than the sum of the thicknesses of the accumulation electron layers, then the exchange interaction between electrons of layers is negligible and the spin polarizations of layers are independent of each other. Let us consider an electron injection from one of the granular films. Injecting electrons are spin polarized by the first accumulation electron layer. After crossing through the first layer, electrons move to the second accumulation layer. If magnetic moments of the accumulation layers are aligned parallel to one another, then moving electrons must surmount the barrier at the distance r_0 from the second interface. In the opposite case, if magnetic moments of the layers are antialigned, then injected spin-polarized electrons must surmount the barrier localized in the region close to the interface plane (figure 3). The height of this barrier is much greater than the height of the barrier at the distance r_0. Thus, the manipulation of magnetic polarizations of the accumulation layers gives rise to an efficient spin-filter effect.

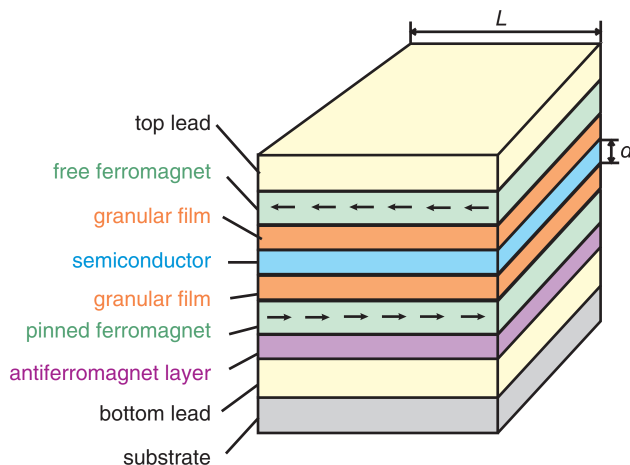

Figure 10. Spin filter on the base of the heterostructure with two granular films with ferromagnetic metal nanoparticles.

We propose a spin filter consisting of the sandwich of two ferromagnetic layers separated by the granular film/SC/granular film heterostructure (figure 10). Magnetic fields of ferromagnetic layers arrange magnetic moments of metal nanoparticles in granular films and polarize accumulation electron layers in the SC. The ferromagnetic layers have different magnetic coercivities to obtain parallel and anti-parallel alignment. In order to manipulate the relative orientation of the magnetic moments of ferromagnets in a more controlled fashion, we can use the structure in which one of the magnetic layers is exchange biased using an antiferromagnetic layer. If the difference of magnetic coercivities of the ferromagnetic layers is small, then these devices display a room temperature spin-filter effect in small magnetic fields. If the size L is small to obtain a single-domain structure, the considered spin filters on the base of the granular film/SC/granular film heterostructure can be regarded as advanced non-volatile magnetic memory storage cells.

4. Conclusion

We have investigated the potential barrier induced by the exchange interaction in the SC/FM heterostructure and have obtained the following results.

(1) It is found that the exchange interaction between electrons in the accumulation layer near the interface in the SC and electrons in the FM forms the potential barrier for injected spin-polarized electrons. The existence of localized electron states in the accumulation layer leads to the increase of the effective exchange interaction and to the increase of the height of the potential barrier. Due to localized states the temperature dependence of the potential barrier height has a maximum. It is found that the barrier height strongly depends on the difference of chemical potentials between the SC and the FM. Maximum values of the barrier are achieved in heterostructures, in which the accumulation layer contains a small number of localized electron states at the interface. Potential barriers in SCs with high electron concentrations ($>10^{19}$ cm^{-3}) have small thicknesses, are tunnel transparent and do not influence spin-polarized injection currents.

(2) In the framework of the developed theoretical model, the injection magnetoresistance effect in SC/granular film heterostructures with ferromagnetic metal nanoparticles is explained as surmounting of injected electrons over the potential barrier. We propose a

spin filter on the base of the granular film/SC/granular film heterostructure operated at room temperature.

Acknowledgment

This work was supported by the Russian Foundation for Basic Research, grant no 06-02-17030.

References

[1] Žutič I, Fabian J and Das Sarma S 2004 *Rev. Mod. Phys.* **76** 323
[2] Zakharchenya B P and Korenev V L 2005 *Phys. Usp.* **175** 603
[3] Bertacco R, Riva M, Cantoni M, Ciccacci F, Portalupi M, Brambilla A, Duo L, Vavassori P, Gustavsson F, George J-M, Marangolo M, Eddrief M and Etgens V H 2004 *Phys. Rev.* B **69** 054421
[4] Wolf S A, Awschalom D D, Buhrman R A, Daughton J M, von Molnar S, Roukes M L, Chtchelkanova A Y and Treger D M 2001 *Science* **294** 1488
[5] Schmidt G 2005 *J. Phys. D: Appl. Phys.* **38** R107
[6] Schmidt G, Richter G, Grabs P, Gould C, Ferrand D and Molenkamp L W 2001 *Phys. Rev. Lett.* **87** 227203
[7] Ohno Y, Yong D K, Beschoten B, Matsukura F, Ohno F and Awschalom D D 1999 *Nature* **402** 790
[8] Jonker B T, Park Y D, Bennett B R, Cheong H D, Kioseoglou G and Petrou A 2000 *Phys. Rev.* B **62** 8180
[9] Hirohata A, Xu Y B, Guertler C M and Bland J A C 2000 *J. Appl. Phys.* **87** 4670
[10] Hirohata A, Xu Y B, Guertler C M, Bland J A C and Holmes S N 2001 *Phys. Rev.* B **63** 104425
[11] Isakovic A F, Carr D M, Strand J, Schultz B D, Palmstrøm C J and Crowell P A 2001 *Phys. Rev.* B **64** 161304
[12] Xiong Z H, Di W, Vardeny Z V and Shi J 2004 *Nature* **427** 821
[13] Hanbicki A T, Jonker B T, Istkos G, Kioseoglou G and Petrou A 2002 *Appl. Phys. Lett.* **80** 1240
[14] Zhu H J, Ramsteiner M, Kostial H, Wassermeier M, Schönherr H-P and Ploog K H 2001 *Phys. Rev. Lett.* **87** 016601
[15] Schmidt G, Ferrand D, Molenkamp L W, Filip A T and van Wees B J 2000 *Phys. Rev.* B **62** R4790
[16] Borukhovich A S 1999 *Phys. Usp.* **42** 653
[17] Kessler J 1985 *Polarized Electrons* (Berlin: Springer)
[18] Hammar P R, Bennett B R, Yang M J and Johnson M 1999 *Phys. Rev. Lett.* **83** 203
[19] Hammar P R and Johnson M 2001 *Appl. Phys. Lett.* **79** 2591
[20] Jiang X, Wang R, Shelby R M, Macfarlane R M, Bank S R, Harris J S and Parkin S S P 2005 *Phys. Rev. Lett.* **94** 056601
[21] Mattana R, George J-M, Jaffres H, Nguyen Van Dau F and Fert A 2003 *Phys. Rev. Lett.* **90** 166601
[22] Lutsev L V, Stognij A I and Novitskii N N 2005 *JETP Lett.* **81** 514
[23] Lutsev L V, Stognij A I, Novitskii N N and Stashkevich A A 2006 *J. Magn. Magn. Mater.* **300** e12
[24] Izyumov Yu A, Kassan-ogly F A and Skryabin Yu N 1974 *Field Methods in the Theory of Ferromagnetism* (Moscow: Nauka)
[25] Abrikosov A A, Gor'kov L P and Dzyaloshinski I E 1975 *Methods of Quantum Field Theory in Statistical Physics* (New York: Dover)
[26] Izyumov Yu A and Medvedev M V 1970 *Sov. Phys.—JETP* **32** 302
[27] Izyumov Yu A, Kassan-ogly F A and Medvedev M V 1971 *J. Physique* **32S** C1 1077
[28] Fomenko V S and Podchernyaeva I A 1975 *Emission and Adsorption Properties of Substances and Materials* (Moscow: Nauka)
[29] Lutsev L V, Kalinin Yu E, Sitnikov A V and Stognei O V 2002 *Phys. Solid State* **44** 1889
[30] Glazman L I and Shekhter R I 1988 *Sov. Phys.—JETP* **67** 163
[31] Glazman L I and Matveev K A 1988 *Sov. Phys.—JETP* **67** 1276